Multi-objective Optimization Framework for Trade-Off Among Pedestrian Delays and Vehicular Emissions at Signal-Controlled Intersections

Görkem Akyol[1,2] · **Sadullah Göncü**[2,4] · **Mehmet Ali Silgu**[3,5]

Abstract

Traffic congestion has several adverse effects on urban traffic networks. Increased travel times of vehicles, with the addition of excessive greenhouse emissions, can be listed as harmful effects. To address these issues, transportation engineers aim to reduce private car usage, reduce travel times through different control strategies, and mitigate harmful effects on urban networks. In this study, we introduce an innovative approach to optimizing traffic signal control settings. This methodology takes into account both pedestrian delays and vehicular emissions. Non-dominated sorting genetic algorithm-II and Multi-objective Artificial Bee Colony algorithms are adopted to solve the multi-objective optimization problem. The vehicular emissions are modeled through the MOVES3 emission model and integrated into the utilized microsimulation environment. Initially, the proposed framework is tested on a hypothetical test network, followed by a real-world case study. Results indicate a significant improvement in pedestrian delays and lower emissions.

Keywords Traffic optimal signal setting · Traffic signal control · Traffic control model · Multi-objective optimization

1 Introduction

Safe and efficient management of signalized intersections is deeply linked to traffic signal control schemes in urban networks. In the literature, numerous studies try to optimize the traffic signal settings [1, 2]. While the optimization schemes may vary, the goals remain consistent for any traffic signal control problem: reducing excessive delays and minimizing emitted vehicular emissions. Generally, traffic signal controls are employed in the intersections in urban centers (i.e., Central Business Districts). Furthermore, these urban centers are also subject to high pedestrian demand. These high pedestrian volumes are inevitably affected by the employed signal control strategies, which aim to mitigate vehicular traffic congestion while causing excessive delays to pedestrians if executed poorly. Traditionally, adjustments to traffic signal control parameters are made exclusively based on the characteristics and attributes of vehicular traffic [3]. Also, in traditional practice, pedestrian green times are exclusively selected to satisfy the minimum pedestrian green time constraints. As the goals of minimizing vehicular and pedestrian delay inherently conflict with each other, a trade-off exists between these two objectives. Ishaque and Noland created a hypothetical network to reveal the trade-off between vehicular and pedestrian delay [4, 5]. In their study, Ishaque and Noland [5] used a priori weights (relative value of time) to evaluate the signal timing settings in mixed traffic conditions. A multiple objective optimization framework is developed in [6] to evaluate vehicle and pedestrian delays. For the optimization of split and cycle durations, a Mixed-Integer Linear Program (MILP) is proposed in [7] to minimize pedestrian

✉ Mehmet Ali Silgu
    masilgu@bartin.edu.tr

    Görkem Akyol
    akyolgo@mef.edu.tr

    Sadullah Göncü
    sgoncu@fsm.edu.tr

1   Department of Civil Engineering, MEF University, 34396 Istanbul, Turkey

2   ITS Research Lab, Technical University of Istanbul, 34469 Istanbul, Turkey

3   Department of Civil Engineering, Bartın University, 74100 Bartın, Turkey

4   Department of Civil Engineering, Fatih Sultan Mehmet Vakıf University, 34445 Istanbul, Turkey

5   Department of Industrial Engineering, Koc University, 34450 Istanbul, Turkey

⚹ Springer

delay while considering the minimum vehicle throughput threshold. A weighted multi-objective optimization problem consisting of pedestrian and vehicular delay is formulated in [8].

In our previous works, [9–11] we proposed a signal control approach to optimize vehicle and pedestrian delays at signalized intersections. In [11], we conducted a case study in Kadıköy, Istanbul, to analyze and improve the pedestrian movement in Central Business Districts (CBDs). Furthermore, we investigated the vehicle and pedestrian traffic in a CBD to make a trade-off between vehicle and pedestrian delay. Preliminary results are shown in these works. Despite examining vehicle and pedestrian movement concurrently, the full potential of computationally efficient optimization algorithms and the environmental impact of transportation, especially vehicular emissions, have not been fully utilized in these studies.

Although the literature on the trade-off between vehicle and pedestrian delays is still being investigated, another issue arises when the case study area is too large or the control period is too long. In this matter, computational efficiency gains importance. For the computationally efficient optimization of traffic signal control settings, heuristic approaches are utilized by many researchers. Vissim-based genetic algorithm optimization of signal timings (VISGAOST) is proposed by Stevanovic et al. [12]. To evaluate different control strategies in urban traffic, a genetic algorithm-based heuristic optimization method is proposed in [13]. Yang and Benekohal [14] exploited genetic algorithm to optimize pedestrian and vehicular delays in an isolated intersection. A meta-heuristic approach to minimize pedestrian and vehicular delays has been proposed in [15]. With the rise of environmental perspectives in transportation planning, emission modeling, and environmentally friendly traffic control studies also have gained momentum. In this context, the selection of the right model for estimating vehicular emissions is an important aspect of environmentally friendly traffic control applications. Greenhouse gas emissions generated from vehicular traffic need to be calculated properly. Several emission models have been proposed for the estimation of vehicular emissions. In this work we have summarized, we only reviewed the emission models that have been employed in traffic control studies involving microscopic traffic simulations. A microscopic emission estimator CMEM is integrated with VISGAOST to assess and reduce vehicular emissions in an urban network [16, 17]. In another study, Vissim is integrated with MOVES to calculate CO2 emissions from the road network [18]. Jamshidnejad et al. [19] proposed an integrated model consisting of microscopic traffic simulation software SUMO and microscopic emission model VT-Micro. Xu et al. [20] integrated Vissim with MOVES to calculate emissions from vehicular traffic. An intelligent traffic control system is proposed to minimize vehicle delay, fuel consumption, and emissions [21]. A meta-heuristic approach minimizing both pedestrian and vehicular delays has been proposed in [15]. Two cost functions have been mathematically modeled for vehicles and pedestrians [15]. The Pareto optimal set is created with Harmony Search and Artificial Bee Colony [15, 22, 23]. Nineteen real-life cases have been studied and improvements in delay times are observed compared to the traffic light control strategies installed at the intersections [15]. In recent years, connected and autonomous vehicles (CAVs) have become present on the roads. In this context, traffic signal control algorithms are developed in the presence of CAVs. Liang et al. [24, 25] proposed a signal phasing and timing optimization problem with connected vehicles and pedestrians. In their study, Liang et al.[24, 25] formalized a compound objective function with weighted pedestrian and vehicular delays. Niels et al. [26] proposed an autonomous intersection control system that integrates pedestrians into the control algorithm along with connected and automated vehicles. The main objective of the proposed signal control system in [26] is that pedestrians cannot wait more than a predetermined waiting time. Another autonomous intersection management system that considers pedestrians, namely, AIM-ped, has been presented in [27]. Max pressure control has been adopted in [27] to calculate the optimal trajectories of vehicles. Liu and Gayah [28] applied a modified version of Max pressure algorithm in the presence of connected vehicles at signalized intersections. Another study conducted in [29] considers the delay equity between individual vehicles from the proposed Max pressure algorithm. Tsitsokas et al. [30] proposed a two-layer adaptive signal control framework that combines the Max pressure algorithm with perimeter control to reduce network-wide congestion.

In summary, in terms of objectives, numerous studies that aim to optimize vehicular delays and emissions have been published in the literature to reduce the total time spent in an urban network. Fundamentally, the trade-off between vehicular delays and pedestrian delays still lies at the heart of many traffic signal control studies mainly because while the traffic signal control applications may reduce vehicular delays, it also causes excessive delays to pedestrians. The multi-objective optimization theory states that if two objectives are conflicting, a Pareto front exists between them. Through this work, we aim to address this trade-off and provide a thorough illustration by hypothetical and real-world case studies.

One of the key contributions of this study is the adoption of a multi-objective optimization framework, which provides multiple solutions instead of a single or compound single objective. This approach allows for a more comprehensive exploration of the optimization problem, enabling decision-makers to consider a range of trade-offs between pedestrian delay and vehicular emissions based on different prioritizations.

With these considerations in mind, the novelty of this presented study is threefold: (i) introducing an optimization scheme for signalized intersections that seeks to minimize pedestrian delays and vehicular emissions instead of vehicular delays, a first to the best of the authors' knowledge, (ii) discuss the potential implications of prioritizing pedestrian delays and vehicular emissions instead of vehicular delays only, (iii) provide a detailed analysis of the trade-off between vehicular delays and pedestrian delays through a real-world case study.

The organization of the paper is as follows: Sect. 1 covers the background information and related literature on traffic signal control and vehicular emissions; Sect. 2 presents the problem formulation, proposed framework, and our solution methodology; then in Sect. 3, properties of our case study and hypothetical network, calibration, and results are illustrated. Finally, conclusions and future research directions are given in Sect. 4.

2 Methodology

In this part, problem formulation, modeling framework, and solution methodology will be given, respectively.

2.1 Problem Formulation

The problem we define involves two conflicting objectives. The initial objective pertains to pedestrian delays at signalized intersections, while the secondary objective concerns vehicular emissions at these intersections. The red signal duration for pedestrians is proportional to the first objective, while the red signal duration for vehicles is proportional to the second objective. This scenario establishes a trade-off between the two objectives. The formulation of the bi-objective optimization problem is provided below.

$$\min \quad f_1(g_p), f_2(g_v) \tag{1}$$

$$\text{s.t.} \quad g_{p,\min} \leq g_p \tag{2}$$

$$g_{v,\min} \leq g_v \tag{3}$$

$$C_{\min} \leq C \leq C_{\max} \tag{4}$$

$$\sum_{i=1}^{N} g_i + L_i = C \tag{5}$$

The objective function in Eq. (1) is composed of two terms: $f_1(g_p)$ which seeks to minimize pedestrian delay, and the second term $f_2(g_v)$ aiming to minimize the total number of stops in one signal cycle. The first constraint in Eq. (2) ensures that the green time allocated for pedestrians is greater than or equal to the minimum pedestrian green time. As in Eqs. (2), (3) ensures that the green time allocated for vehicles

must be greater than or equal to the minimum vehicle green time. The constraint in Eq. (4) delineates the boundaries for cycle length duration. Equation (5) details the components of one signal cycle, where $g_{p,\min}$ represents the minimum pedestrian green time, $g_{v,\min}$ represents the minimum vehicle green time, the minimum cycle length is denoted by $C_{\min}$, maximum cycle length is denoted by $C_{\max}$, and L_i is the lost time occurring at each phase i. The decision variables are designated as g_p and g_v where g_p represents pedestrian green time, and g_v represents vehicle green time. The first objective function, which encompasses pedestrian delay at signalized intersections and is adopted from the [31], is given in Eq. (6)

$$f_1(g_p) = q_p * \frac{(C - g_p)^2}{2C} \tag{6}$$

In Eq. (6), q_p represents the pedestrian volume in one cycle, and other parameters are previously defined. The second objective function utilizes Akcelik's number of stops function [32].

$$f_2(g_v) = \sum_{i=1}^{N} \frac{q_v * (1 - \lambda_i) * (\sum_{i=1}^{N}(g_i + L_i))}{(\sum_{i=1}^{N}(g_i + L_i) * (1 - \frac{q_v}{s_i})} \tag{7}$$

In Eq. (7), s_i represents the saturation flow rate, q_v is the mean arrival rate of vehicles, and λ_i is the green time ratio of phase i.

Under uniform vehicle arrivals, an increase in pedestrian green time (g_p) leads to a reduction in pedestrian delay, but it comes at the expense of an increase in the total number of stops. Therefore, a trade-off exists between these two objectives, and we aim to illustrate and analyze this trade-off. In the subsequent sections, we will show the non-dominated solutions of the problem by using a non-dominated sorting genetic algorithm (NSGA-II) [33] and a multi-objective artificial bee colony [23] (MOABC) algorithm. Calculation of the minimum pedestrian green time for pedestrians is adopted from Mannering and Washburn [34], and it reads:

$$g_{p,\min} = 3.2 + \frac{L}{S_p} + 0.27 N_{\text{ped}} \qquad \text{for } W_e \leq 3\text{m} \tag{8a}$$

$$g_{p,\min} = 3.2 + \frac{L}{S_p} + (2.7 \cdot \frac{N_{\text{ped}}}{W_e}) \quad \text{for } W_e \geq 3\text{ m} \tag{8b}$$

In Eq. (8a) L stands for crosswalk length, S_p stands for the pedestrians' average walking speed, N_{ped} is the number of pedestrians crossing the road during the green phase, and W_e stands for the effective crosswalk width. In our case, all the effective crosswalk widths are greater than 3 ms; therefore, Eq. (8b) is used for the calculation of minimum pedestrian green time. Selection of the parameters in our case is as follows: Effective crosswalk width W_e is measured as 3.1 ms,

length of crosswalk L is 7 ms, average pedestrian speed S_p is 1.3 ms, and average number of pedestrians passing during the green phase N_{ped} is measured as 19 pedestrians. In our methodology, minimum pedestrian green time is determined as 24 s, minimum green time for vehicles is selected as 40 s, minimum cycle length is selected as 84 s, and maximum cycle length is selected as 160 s.

2.2 Modeling Framework

In this sub-section, we present the utilized framework for modeling vehicular and pedestrian traffic, together with the employed emission models. Additionally, the integration of simulation environment and emission models is given.

For our deterministic study, the following traffic network assumptions have been considered: (i) Network entrance and exit flows are known, (ii) turning ratios at the intersections are known, (iii) delay for vehicles occurs only by traffic signals, (iv) the number of waiting and crossing pedestrians at each side of the crosswalk are known during all the simulation, (v) number of pedestrians and their diversion ratios in their route are known a priori.

Vehicles' movement on the links and intersections is modeled by adding additional constraints to our optimization problem. For the problem at hand, since we are dealing with traffic signal control, phase status constraints and conservation of vehicles principle are considered. Phase status constraints for an intersection I are that there exists only one active phase for each sampling interval k. The formulation of phase status constraints is as follows:

$$(\forall i \in \varphi_I)\omega_i(k) = 0 \Rightarrow (\forall(m, n \in \vartheta_I(i))q_{mn}(k) = 0 \quad (9a)$$

$$\sum_{i \in \varphi_I} \omega_i(k) = 1 \quad (9b)$$

$$(\forall i \in \varphi_I)(\forall k \in \mathbb{N})\omega_i(k) \in \{0, 1\} \quad (9c)$$

where $\omega_i(k) = 0$ and $\omega_i(k) = 1$ indicate the "RED" and "GREEN" traffic signal associated with the phase i, respectively, and $\mathbb{N}$ denotes the natural number set. Sub-script i denotes the phase in the intersection I, φ_I denotes the set of phases in intersection I, $\omega_i(k)$ is the traffic signals associated with the phase i at the sampling interval k, $\vartheta_I(i)$ represents the association of each phase to relevant compatible stream, $q_{mn}(k)$ is the number of vehicles exiting the link m to n in the interval k. Equation (9a) indicates that if the traffic signal at phase i of intersection I is RED in interval k, there will be no vehicles passing at that phase; therefore, $q_{mn}(k) = 0$. In Eq. (9b, it can be seen that there can be only one GREEN traffic phase at any time interval k.

Due to the vehicle flow conservation principle, each link m in the system has the following volume dynamics:

$$Q_m(k + 1) = Q_m(k) + v_m(k) - v_m(k), \quad (10)$$
$$(\forall k \in \mathbb{N})Q_m(k) \in \mathbb{N}$$

where $Q_m(k)$ is the number of vehicles in link m at the sampling interval k, $v_m(k)$ is the inflow on link m at the time interval k, and $v_m(k)$ is the outflow on link m at the time interval k.

In terms of the simulation environment, we have encountered its user-friendly features in various prior studies related to freeway traffic modeling, such as state modeling [35], addressing the control challenges of freeway ramps [36, 37], as well as urban road flow modeling [38]; we opted to utilize PTV Vissim [39]. PTV Vissim provides a multi-modal traffic modeling capability together with a user-friendly interface. Vehicular traffic simulations are based on Wiedemann's car-following model for urban traffic [40]. The pedestrian simulation model incorporates the Social Force Model which is proposed by Helbing and Molnar [41].

Vissim can provide a large set of utilities by the Component Object Model (COM) feature. Through the COM interface, we can dynamically alter the capabilities of Vissim, integrate various signal control programs, and interfere with vehicle routes, trajectories of vehicles, and pedestrians. The COM interface also facilitates the connection between Vissim and MATLAB, allowing for optimization to be performed in MATLAB and the implementation of solutions in Vissim.

In terms of estimating vehicular emissions, we employ the MOVES3 [42] emission model, which is a state-of-the-art estimation tool with an open-source code. MOVES3 allows three different scales for users to model the emissions: (i) national, (ii) county, and (iii) project. National and county scales are used for macroscopic assessment of emissions, whereas project scale is used for microscopic assessment. Trajectory data of each vehicle are used in the project scale. Instantaneous (second-by-second) speed and acceleration data can be obtained by the Vissim COM feature and can be used as an input for emission calculation.

MOVES3 uses operating modes of vehicles which is incorporated by their instantaneous speed and acceleration values. The operating mode distribution allows the user to enter vehicle activity data for each second as a function of vehicle-specific power (VSP). VSP is the key concept for the calculation of running emissions, and it is an estimate of the power demand on the engine during driving. VSP can be calculated for each second and each vehicle as given in Eq. (11).

$$\text{VSP}_t = \frac{Av_t + Bv^2 + Cv^3 + mv_t(a_t + g\sin(\theta_t))}{m} \quad (11)$$

Raw trajectory data obtained from Vissim are not ready to be handled by MOVES3. By using Eq. (11), VSP for each vehicle needs to be calculated for each second. After calculating the VSP, operating mode bins for each vehicle need to be assessed from the operating mode distribution table. Occurrences for all vehicle types and operating mode ID combinations are counted to create an operating mode fraction. Afterward, pollutant process IDs need to be assigned for each operating mode ID. For the last step, the MOVES3 default database gives the relationship between pollutants and associated operating mode bins.

The general architecture for the proposed framework can be found in our previous study [43]. In this context, MATLAB serves two primary purposes: i) optimizing signal control settings and (ii) interacting with Vissim through the COM interface. Due to the conflicting multi-objective structure of our objective function, the proposed framework yields more than one solution. The employed COM interface enables the retrieval of the number of vehicles and pedestrians in specific links on our networks, allowing us to dynamically adapt the signal control program. This feedback loop is repeated every 10 min, and upon completion of the simulation trials, vehicle trajectories are extracted from Vissim and input into the MOVES3 emission tool.

2.3 Solution Methodology

Multi-objective optimization problems hold more than one feasible solution. In feasible region set S, there are vectors that cannot improve any of the components without deteriorating to at least one of the other components [44]. Pareto optimality is named after French-Italian economist Vilfredo Pareto who used the concept of Pareto optimality [45]. Pareto optimality is defined below: A decision vector $x^* \in S$ is Pareto optimal if no other decision vector $x \in S$ exists with the following conditions:

1. $f_i(x) \leq f_i(x^*)$ for all $i = 1, ..., k$ and
2. $f_j(x) < f_j(x^*)$ for at least one index j.

A objective vector $z^* \in Z$ is Pareto optimal if no other objective vector $z \in Z$ exists with the following conditions:

1. $z_i \leq z_i^*$ for all $i = 1, ..., k$ and
2. $z_j < z_j^*$ for at least one index j.

An evolutionary algorithm NSGA-II [33] and Multi-objective Artificial Bee Colony (MOABC) [23] are adopted for our solution method. NSGA-II is a fast and elitist multi-objective genetic algorithm. Multiple Pareto optimal solutions can be acquired from a single simulation run [33]. The main loop of the NSGA-II initiates with genetic algorithm operators such as selection, crossover, and mutation to create an offspring population Q_t with the same number of solutions N. The two populations are merged to form a new population with size 2N called R_t. The sorting process is applied to categorize the entire population R_t. The current population and the offspring population are evaluated together. Good solutions found in the current population are kept to enable elitism.

ABC is a population-based meta-heuristic algorithm that was developed by Karaboga [23]. MOABC is developed through the literature and used extensively [15, 46–48]. MOABC operates based on the intelligent behavior of a honey bee swarm and employs three distinct types of bees within the ABC algorithm: employed bees, onlooker bees, and scout bees. Employed bees are responsible for exploiting a food source, onlooker bees wait in the hive to select a food source, and scout bees engage in a random search for new food sources. In this context, food sources symbolize solutions to the problem, and the fitness of each solution is linked to the amount of nectar associated with the corresponding food source.

The schematic diagram for MOABC is presented in Fig. 1. During the initialization phase, algorithm parameters such as the number of food sources, the threshold for abandoning a food source after a specified number of trials, and termination criteria are defined. Notably, the count of food sources denoted as (SN) aligns with the number of employed bees, and this count is equivalent to the number of onlooker bees. The population is initiated by randomly generating food sources, where each source is represented by an n-dimensional real-valued vector.

Let x_i represent the ith food source in the population. The process for generating random food sources is outlined as follows:

$$x_{ij} = x_{ij}^{\min} + r \times (x_j^{\max} - x_j^{\min}), i = 1, 2, ..., SN,$$
$$\text{and } j = 1, 2, ..., n \tag{12}$$

where r is a uniform random number in the range of [0, 1]. $x_j^{\min}$ and $x_j^{\max}$ are the lower and upper boundaries for dimension j, respectively. Employed bees are assigned to food sources randomly, and corresponding fitness is evaluated. In the employed bee phase, each employed bee x_i generates a new food source X_{new} near its current position as follows:

$$x_{\text{new}(j)} = x_{ij} + r' \times (x_{ij} - x_{kj}) \tag{13}$$

$k = 1, 2, ..., SN$ and r' represents randomly chosen indexes with r' being a randomly distributed real number in $-1, 1$, a new solution X_{new} is computed. This newly calculated solution X_{new} is then compared to the existing solution X_i. If the fitness value of X_{new} is greater than or equal to the fitness value of X_i, X_{new} replaces X_i as a new food source. Otherwise, X_i is retained in the archive.

In the onlooker bee phase, all employed bees undergo evaluation by an onlooker bee. Subsequently, a food source X_i is selected based on its probability value p_i, which is computed as follows:

$$p_i = \frac{f_i}{\sum_{i=1}^{SN} f_i} \tag{14}$$

where f_i is the nectar amount of fitness value of the ith food source. The selection chance of ith food source is proportional to the value f_i. Once the food source X_i is selected, one onlooker bee updates X_i by using Eq. 13. If the new food source has equal or better fitness value than X_i, the new food source replaces X_i as a new member in the population.

In the scout bee phase, food source X_i is to be abandoned if it cannot be improved through a predetermined number of trials. Next, the corresponding employed bee becomes a scout bee and it produces a new food source randomly as follows:

$$x_{ij} = x_j^{\min} + r \times (x_j^{\max} - x_j^{\min}), j \in \mathbb{N} \tag{15}$$

This procedure continues until a termination criterion is satisfied.

Initially, the Pareto optimal solutions are obtained using the NSGA-II and MOABC, and results are fed into the signal control program. Although the solutions obtained from evolutionary algorithms are near-optimal compared to classical methods, the proposed approach provides less computational time, and the usage of unbiased weights compensates for the drawbacks.

For the given problem, the parameters for NSGA-II and MOABC are specified as follows. The number of generations is capped at 200. A crossover rate of 0.5 is chosen, along with a mutation probability of 0.03. The convergence threshold is set to 0.001. These parameters are chosen because of their common usage in the literature [14, 16, 49, 50]. For the MOABC algorithm, the population size is set to 100. The number of generations is set to 1000, and the maximum number of trials is set to 50 [46, 47, 51].

As explained in our methodology, we have two objective functions. The first one is for pedestrian delay; the second one is for the number of stops by vehicles. Through the NSGA-II and MOABC algorithms, we have obtained the Pareto optimal solutions for our cases. The results are presented in Fig. 2.

In the left side of Fig. 2, black and magenta points show the decision variable space where each point corresponds to a signal control program. In addition, black and cyan points on the right side of Fig. 2 represent the Pareto optimal solutions together with the true Pareto front.

The results depicted in Fig. 2 reveal that both the NSGA-II and MOABC algorithms effectively discern a genuine Pareto front associated with two opposing objectives—specifically,
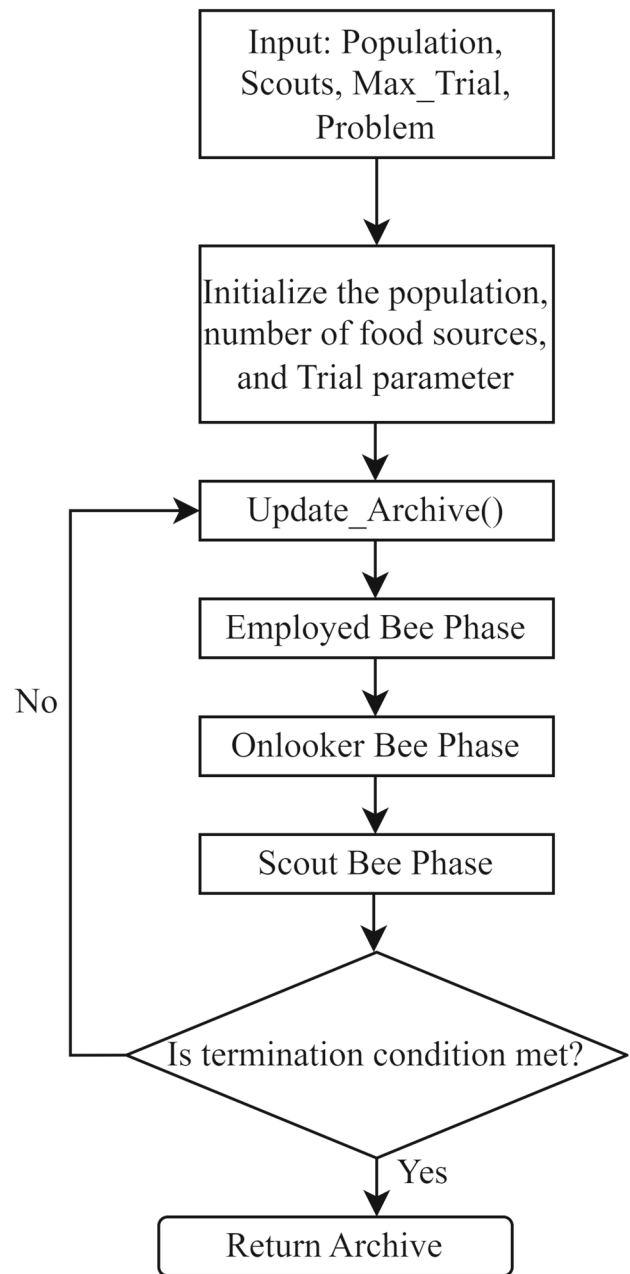

Fig. 1 Schematic diagram of the MOABC algorithm

pedestrian delay and vehicular emissions (represented by the total number of stops). Depending on the prevailing traffic conditions, the optimization framework can offer solutions that simultaneously minimize pedestrian delay and the total number of stops to varying extents. This aligns with the overarching goal of the proposed framework (Fig. 3).
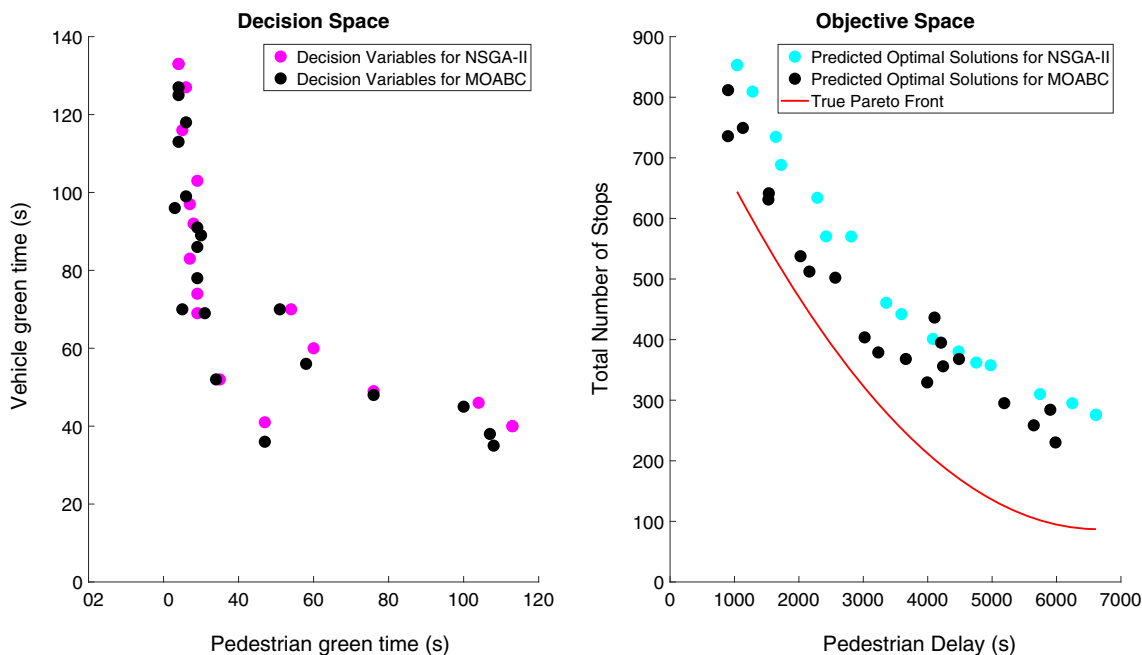
Fig. 2 Objective and decision space together with true Pareto front

3 Case Study

The proposed framework is tested through two microsimulation-based case studies: on a hypothetical intersection with synthetic data, and a real-world intersection with field measurements. Before the properties of real-world and hypothetical case studies are given, the calibration procedure of the simulation model is given in the next subsection.

3.1 Calibration of Simulation Model

Before a simulation is performed, calibration of the simulation model needs to be done. The calibration aims to minimize the difference between reality and the simulation model. GEH statistic [52] is selected as the measure considered in calibration. GEH statistic is defined in Eq. 16.

$$\text{GEH} = \sqrt{\frac{2(y - x)^2}{y + x}} \tag{16}$$

Before conducting a simulation, calibration of the simulation model is essential. The calibration process seeks to minimize the disparity between reality and the simulation model. The chosen measure for calibration is the GEH statistic [52], defined in Eq. 16.

Figure 4 illustrates the temporal variations of GEH statistics at two intersections of interest. As observed from Fig. 4, the calculated GEH values for each intersection are consistently lower than the predefined value, accounting for approximately over 90% of the time.
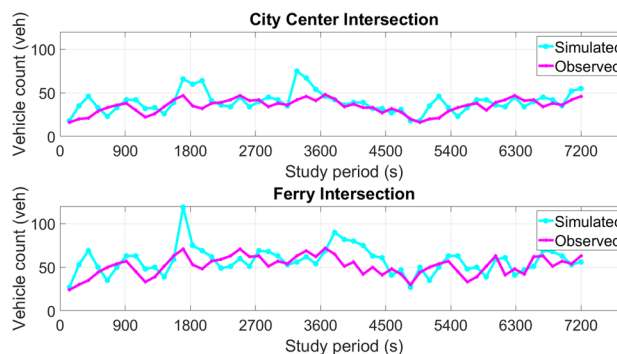

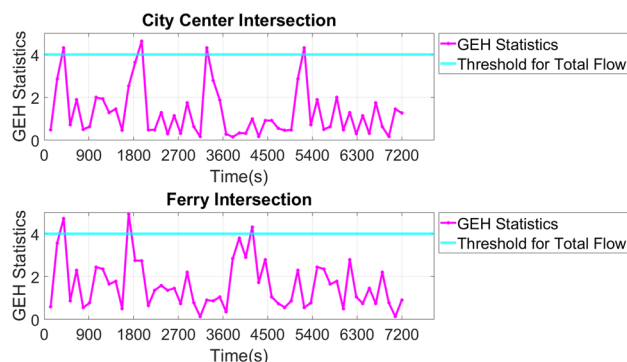**Fig. 3** Actual versus model values from simulation of traffic flows

Fig. 4 Variation of GEH statistics obtained through calibration

3.2 Real-world and hypothetical case studies

For the real-world case study, we have chosen the Kadıköy district in Istanbul. Residents can access the case study area using various modes of transportation, including private cars, buses, minibuses, metrobus (bus rapid transit), metro, and ferries from multiple locations. Additionally, a historical tram line runs through the inner parts of Kadıköy and the coastal area.

The field measurements involve capturing footage from cameras positioned on two high-rise buildings. We have employed this footage to analyze pedestrian and vehicular movements within two distinct time intervals: 12:00–14:00 and 17:30–19:30. In Fig. 5, the depicted case study area highlights the pedestrians' open walking spaces in light orange polygons. Additionally, green arrows signify the locations of ferry stations, and a two-headed dark blue arrow points to the traffic lights and crosswalks under investigation in this research. The northern end of the dark blue arrow designates the crosswalk closer to the ferry terminals, while the southern end indicates the crosswalk nearer to the central area of Kadıköy. In this study, the intersection at the northern end of the dark blue arrow is termed the ferry intersection, while the southern end is referred to as the city center intersection.

Although the subject area has several signalized intersections close to each other, we mainly focus on two of these signalized intersections. Considered signalized intersections are located at the heads of the green arrow in Fig. 5. These two signalized intersections have identical parameters, and the signal control program consists of four phases. The first phase is the green light for vehicles where the pedestrians wait at the red phase. The second phase is all-red for all traffic units. The third phase is green signal duration for pedestrians and the last phase is all-red. Cycle length is 110 s, green signal duration for vehicle traffic is 75 s, green signal duration for pedestrian traffic is 15 s, and all-red signal duration is 10 s in the case study area. In the hypothetical case, we used the same signal timing parameters for comparison.

Since Kadıköy is an urban area, the speed limit of 50 km/h is selected as the desired speed for simulation trials. To provide a more reliable result, simulations are carried out with 10 different random seeds, and the presented results are the averages of trials. Every simulation is executed in real-time duration, one simulation second corresponds to one second in real time.

The hypothetical case study consists of 4 intersections connected. Every approach has two lanes for incoming and two lanes for outgoing directions. As the microsimulation environment, PTV Vissim is employed. A general overview of the hypothetical case and phase diagram used is presented in Fig. 6. Dotted lines show pedestrian movement, whereas solid lines are represented for vehicular movement. No exclusive pedestrian phase is used. For the simulation

of pedestrians, an add-on module, PTV Viswalk is used. In the signal phasing program for our hypothetical case, there are four phases. At each phase, only one approach (eastbound, northbound, westbound, southbound, respectively) can move along its direction. In the hypothetical scenarios, we loaded 3000 vehicle-per-hour (vph) to the network in high flow input, 2000 vph in medium flow input, and 1000 vph in low vph input. In the high flow input, 500 vph is loaded for North–South and South-North directions; meanwhile, 1000 vph is loaded for East–West and West-East directions. For the medium flow input, 333 vph is loaded for North–South and South–North directions; meanwhile, 667 vph is loaded for East–West and West–East directions. For the low flow input, 166 vph is loaded for North–South and South-North directions; meanwhile, 334 vph is loaded for East–West and West-East directions. For our four-phase signal program, phase one and phase three have 30 s of green duration, and phase two and phase four have 15 s of green duration. All-red duration for this particular program is set to 5 s. In total, the cycle length is equal to 110 s for all cases.

The case study area consists of 70 links for vehicular traffic and a total of 16 areas for pedestrian activity. Throughout the case study corridor, 13 signalized intersections are modeled and all of these intersections are subject to pedestrian flow as well. The simulation environment for the real-world network modeled in Vissim can be seen in Fig. 7. Gray areas show the vehicular network, while cyan areas show the pedestrian activity zones.

3.3 Webster Method and Its Application

In his pioneer work, Webster [53] formulated the optimal cycle time on signal-controlled intersections. Before the calculation of optimum cycle length, critical lane flows and saturation lane flows should be known. Considering Fig. 6, critical lane flows are as follows:

$$y_1 = \frac{\max((1+2),(3+4))}{S_i} \tag{17a}$$

$$y_2 = \frac{\max(5,6)}{S_i} \tag{17b}$$

$$y_3 = \frac{\max((7+8),(9+10))}{S_i} \tag{17c}$$

$$y_4 = \frac{\max(11,12)}{S_i} \tag{17d}$$

where y_i denotes the maximum ratio of flow to saturation flow for a given phase i and S_i denotes the saturation flow. The optimum cycle length calculation according to Webster method reads:

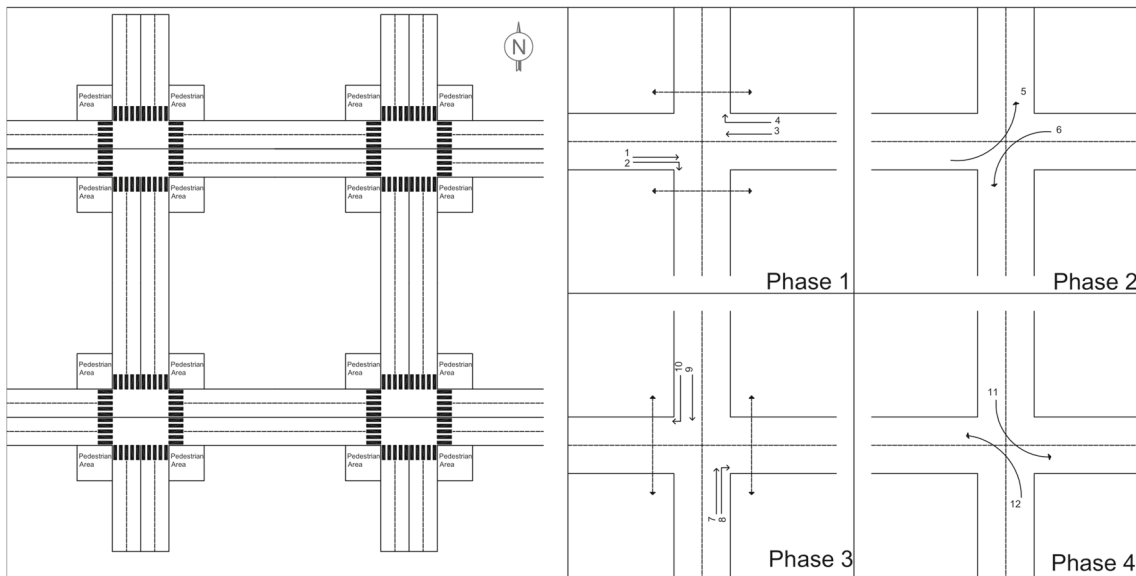$$C_o = \frac{1.5L+5}{1-\sum_{i=1}^{N} y_i} \tag{18}$$

Fig. 5 Case study area

Fig. 6 Hypothetical case phase, **a** 2x2 grid network; **b** phase diagram

where L is lost time that occurs at each phase i and C_o is the optimum cycle length.

3.4 Scenarios Tested

We designed two main scenarios for both hypothetical and real-world cases. In the first scenario, vehicle flows are varied at low, medium, and high levels, with high vehicular flow representing the base case observed in the field survey. In the second scenario, signal control settings are dynamically altered through the COM interface. This second scenario comprises three sub-scenarios: (i) pedestrian priority signal control, (ii) balanced signal control, and (iii) vehicle priority signal control. Within each sub-scenario, priorities are adjusted by modifying the split and cycle durations at each intersection. Pareto optimal solutions are obtained without

Table 1 Flow-related scenario feature

Prioritization	VPH		
	Low (1000 vph)	Medium (2000 vph)	High (3000 vph)
Pedestrian Priority	Pedestrian—Low	Pedestrian—Medium	Pedestrian—High
Balanced	Balanced-Low	Balanced-Medium	Balanced-High
Vehicle Priority	Vehicle-Low	Vehicle-Medium	Vehicle-High
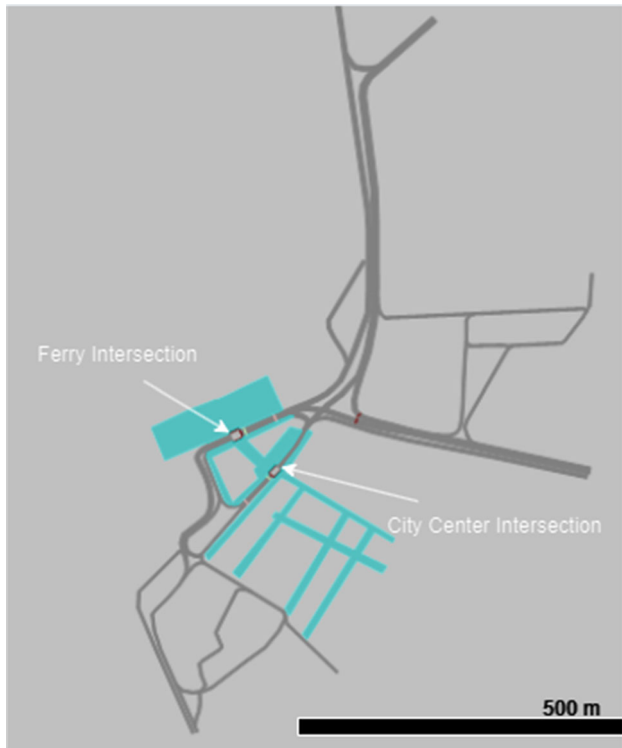
Fig. 7 Simulation environment in Vissim

assigning any weight to the objective functions, allowing us to prioritize objectives based on the results.

Table 1 shows the scenario properties explained above. Pedestrian volume is kept at the same level (720 pedestrians per hour per direction for each intersection) in all scenarios to investigate the effects of vehicle flow on intersection performance.

Priority scenarios are as follows: Pedestrian—High describes that there is high vehicular flow in the network (3000 vph) and priority is given to the pedestrians. In the Pedestrian—Medium sub-scenario priority is given to pedestrians, while the network is loaded with 2000 vph. In Pedestrian—Low, there is 1000 vph in the network with pedestrian priority. In Balanced sub-scenarios, the difference between vehicle and pedestrian green times is minimized. Lastly, in Vehicle sub-scenarios, priority is given to vehicles over pedestrians by adjusting vehicle green times with a higher proportion compared to pedestrian green times.

In the Ferry intersection, 700 vph is traversing the intersection through movement in Low vph scenarios, 1500 vph is traversing the Ferry intersection in Medium vph scenarios, 2300 vph is crossing the Ferry intersection in High vph scenarios. For the City center intersection, these values are 500 vph for through and right-turning movement in Low vph scenarios, 1000 vph for through and right-turning movement in Medium vph scenarios, and lastly, 1800 vph is traversing through and turning right in High vph scenario.

3.5 Results and Discussion

In base case scenarios, the cycle length is fixed at 110 s. As explained before, the decision variables were pedestrian green time, g_p, and vehicle green time g_v. Selected green signal duration intervals after the optimization are illustrated in Fig. 8. Scenario and sub-scenario columns show the priority scenarios given in Table 1. Vehicle split and pedestrian split values are chosen from the solutions obtained through our proposed framework. All-red interval is an interval that has a red-signal display before the display of green for the following phase [54].

Solutions applied with the MOABC algorithm indicate lower values compared to NSGA-II results. In pedestrian priority scenarios, vehicular delays and consecutively vehicular emissions increase at the expense of increasing pedestrian throughput. We selected a narrow interval for split durations to mitigate the potential negative impacts of substantial changes in signal control parameters. Adaptive traffic signal control algorithms, such as SCOOT and SCATS, operate similarly in determining split duration changes following optimization.

In all scenarios and cases (hypothetical and real-world), our proposed framework found Pareto optimal solutions for our problem. For the calculation of emissions, vehicle trajectory output is gathered from Vissim at the end of each simulation. After that, emission calculations are done with MOVES3. The summary of results for hypothetical and real-world case studies is illustrated in Fig. 9. As evident from Fig. 9, both NSGA-II and MOABC algorithms demonstrate a notable reduction in pedestrian delay while managing to limit the rise in emitted emissions to a certain extent, in contrast to scenarios with no control and using the Webster method. With the escalation in vehicular demand, emissions from the vehic-
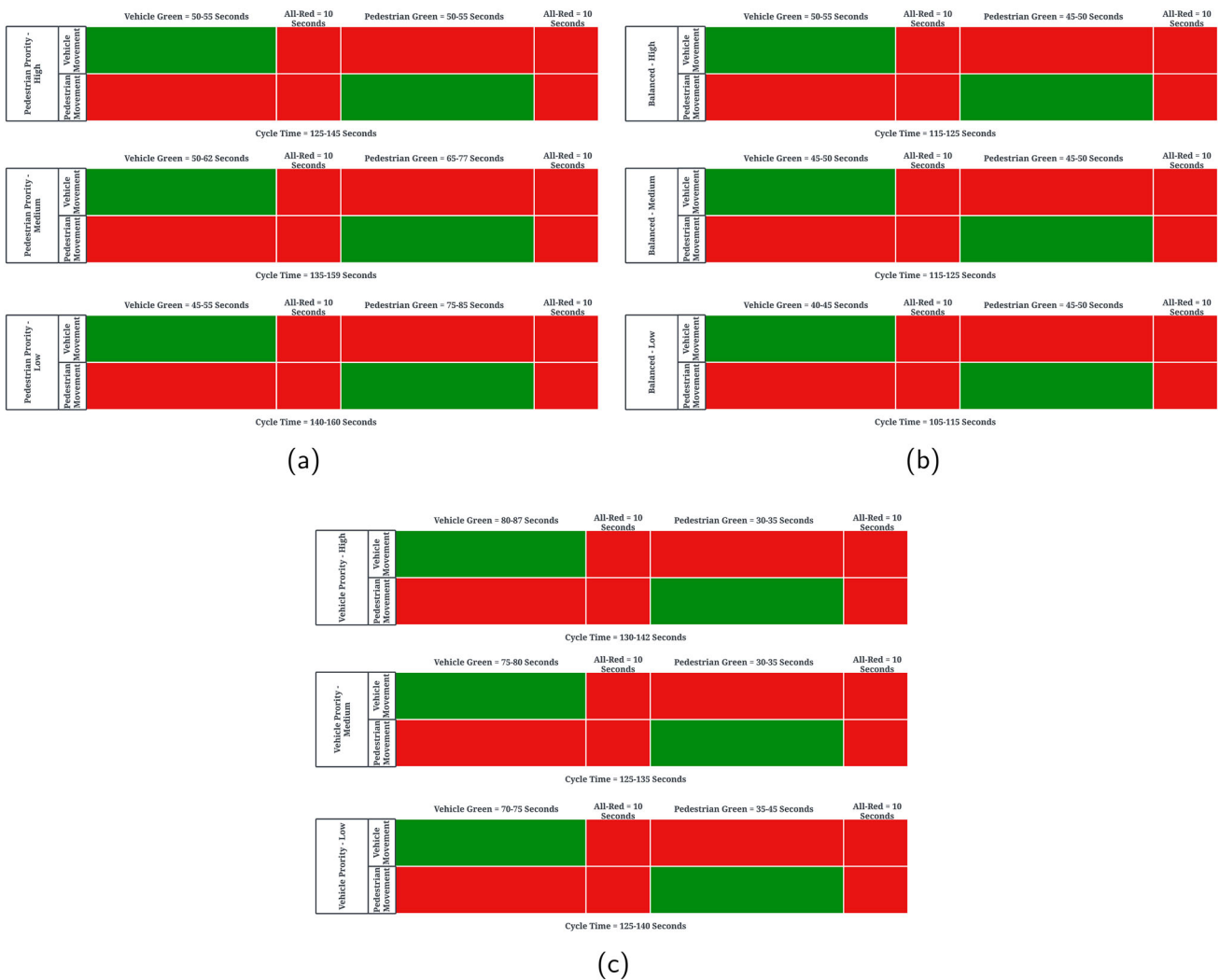
Fig. 8 Green signal durations for scenarios **a** pedestrian priority; **b** balanced; **c** vehicle priority

ular traffic naturally increase. However, when compared to scenarios without control measures, a lower level of emissions is achieved, aligning with the primary objective of the proposed framework. Particularly in Balanced-Medium and Balanced-High scenarios, both delays and emissions exhibit a substantial decrease, approximately ranging from 40 to 50%, compared to the No control cases with similar demand characteristics.

To compare the solution algorithms' effectiveness, a performance metric widely used to evaluate the multi-objective optimization algorithms, namely Inverted Generational Distance (IGD) is used. Let K^* be a set of uniformly distributed points in the Pareto front, while K is the set of non-dominated solutions by each compared algorithm. The IGD [55] is defined as follows:

$$\text{IGD}(K^*, K) = \frac{\sum_{t \in K^*} d(t, K)}{|K|} \tag{19}$$

where $d(t, K)$ is the minimum Euclidean distance in the objective t and the points K. A lower value of IGD states that K is closer to the Pareto front. The IGD value of MOABC resulted in 0.014, while this value is higher for NSGA-II, 0.058. Calculations for the IGD values of both NSGA-II and MOABC indicate that MOABC has better performance in terms of quality of solutions. This finding is consistent with the literature [15, 56].

Since our optimization algorithms do not explicitly optimize vehicular delays, we tabulated the resulting vehicular delay for each case in our real-world case studies for NSGA-II and MOABC in Table 2. In Base Case (No Control) scenarios, there is no signal control program applied externally. In Base Case (Webster) scenarios, optimized signal control settings found by the Webster method were applied to the intersection signal control program.
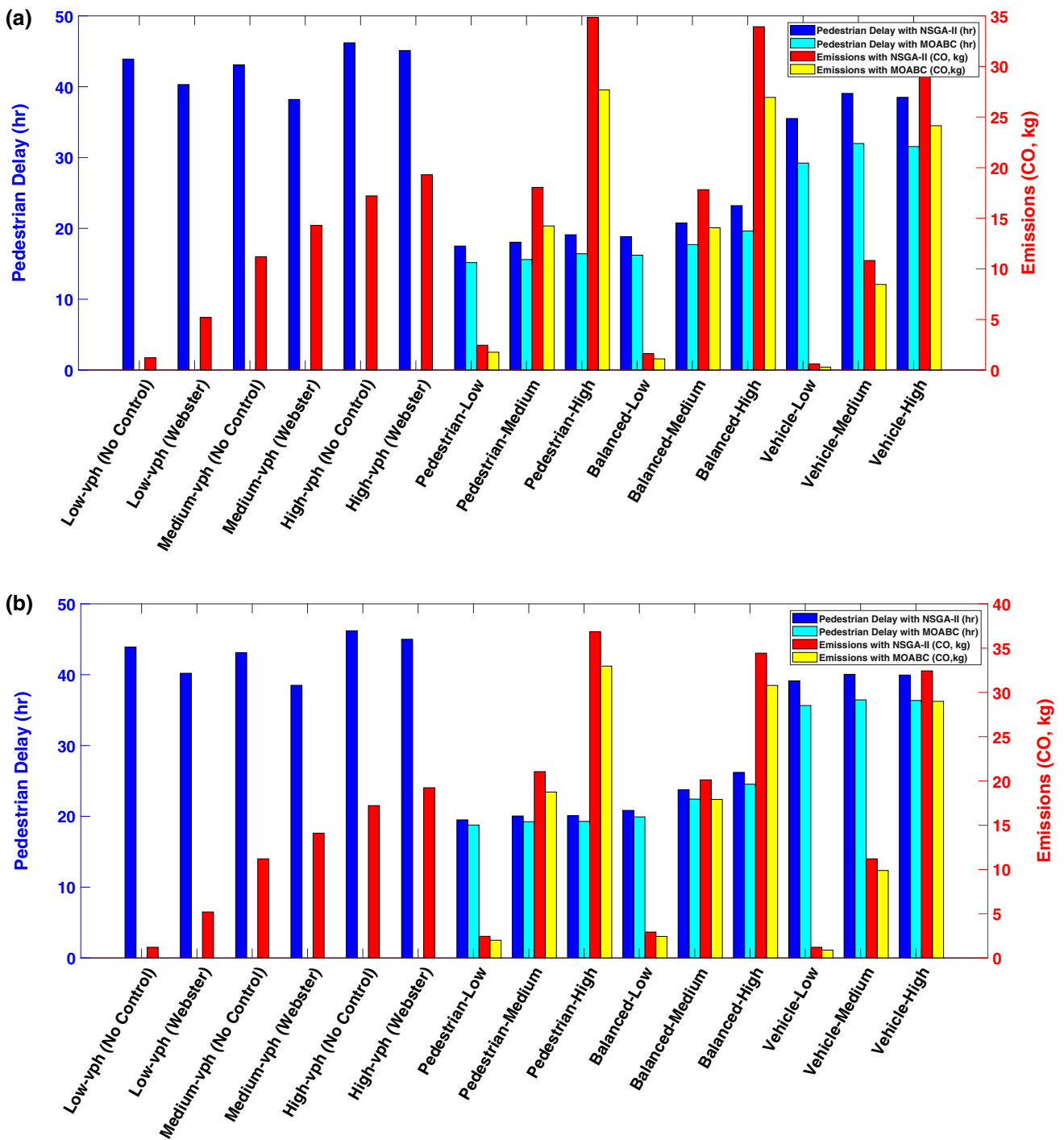
Fig. 9 Results from **a** hypothetical case; **b** real-world case study

4 Conclusions and Future Research

In this study, we have developed an integrated methodology for optimizing traffic signal control, taking into account both pedestrian delay and vehicular emissions. Vissim is chosen as the microscopic traffic simulator, NSGA-II and MOABC are employed to solve multi-objective optimization problems, and MOVES3 is selected to calculate vehicular emissions at a microscopic scale. To assess the proposed framework, hypothetical and real-world case studies are conducted in Kadıköy, Istanbul. Two main scenarios are designed to evaluate the method under varying demand and different prioritization of traffic units. The results demonstrate that the proposed approach can reduce pedestrian delay by up to 59.48%, and emissions are decreased by up to 7.12% compared to the base case. It is evident from the results that pedestrian delay

Table 2 Vehicular delay for our case study

Low Vph	Vehicular Delay with NSGA-II (hr)	Vehicular Delay with MOABC (hr)
Base Case (No control)	42.71	42.71
Base Case (Webster)	44.25	44.25
Pedestrian—Low	23.40	15.84
Balanced—Low	24.20	18.60
Vehicle—Low	44.40	33.67
Medium Vph		
Base Case (No control)	41.86	41.86
Base Case (Webster)	46.53	46.53
Pedestrian—Medium	18.82	16.56
Balanced—Medium	22.26	20.69
Vehicle—High	37.79	31.74
High Vph		
Base Case (No control)	44.26	44.26
Base Case (Webster)	49.84	49.84
Pedestrian—High	24.77	16.64
Balanced—High	29.08	22.54
Vehicle—High	48.68	31.45

improves in all scenarios, while vehicular emissions exhibit fluctuations. Additionally, vehicular delays in the network are also illustrated to see the effects of our proposed method on the traffic network. The solutions obtained from the MOABC algorithm give better results compared to the NSGA-II algorithm in terms of pedestrian delay and vehicular emissions.

The method proposed in this research does not optimize a single objective or a weighted compound single objective. Instead, it addresses a multi-objective optimization problem. This approach means that after the multi-objective optimization process, multiple solutions are obtained instead of a single one. The weights or prioritization are applied post-optimization, providing a flexible way to interpret and address the nuances of the problem at hand.

As future research directions, an extension of the case study and simulation model could be contemplated. Currently, the study focuses on only two traffic signals. Expanding the proposed framework to test various networks and traffic conditions would contribute to its validation. Additionally, the inclusion of different traffic units such as bicycles, buses, in the simulation model and optimization framework could enhance the comprehensiveness and applicability of the proposed methodology.

References

1. Erdagi, I.G.; Dobrota, N.; Gavric, S.; Stevanovic, A.: Cycle-by-cycle delay estimation at signalized intersections by using machine learning and simulated video detection data. In: 2023 8th International Conference on Models and Technologies for Intelligent Transportation Systems (MT-ITS), pp. 1–7, IEEE (2023).
2. Gavric, S.; Dobrota, N.; Erdagi, I.G.; Stevanovic, A.; Osman, O.A.: Estimation of arrivals on green at signalized intersections using stop-bar video detection. Transp. Res. Rec. **2677**(6), 797–811 (2023)
3. Gavric, S.; Sarazhinsky, D.; Stevanovic, A.; Dobrota, N.: Development and evaluation of non-traditional pedestrian timing treatments for coordinated signalized intersections. Transp. Res. Rec. **2677**(1), 460–474 (2023)
4. Ishaque, M.M.; Noland, R.B.: Multimodal microsimulation of vehicle and pedestrian signal timings. Transp. Res. Rec. **1939**(1), 107–114 (2005)
5. Ishaque, M.M.; Noland, R.B.: Trade-offs between vehicular and pedestrian traffic using micro-simulation methods. Transp. Policy **14**(2), 124–138 (2007)
6. Ma, W.; Liu, Y.; Head, K.L.: Optimization of pedestrian phase patterns at signalized intersections: a multi-objective approach. J. Adv. Transp. **48**(8), 1138–1152 (2014)
7. Zhang, Y.; Su, R.; Zhang, Y.: A macroscopic propagation model for bidirectional pedestrian flows on signalized crosswalks. In: 2017 IEEE 56th Annual Conference on Decision and Control (CDC), pp. 6289–6294, IEEE (2017)
8. Yu, C.; Ma, W.; Han, K.; Yang, X.: Optimization of vehicle and pedestrian signals at isolated intersections. Transp. Res. Part B Methodol. **98**, 135–153 (2017)
9. Akyol, G.; Silgu, M.A.; Celikoglu, H.B.: Pedestrian-friendly traffic signal control using eclipse sumo. In: Proceedings of the SUMO User Conference, pp. 101–106 (2019)
10. Akyol, G.; Erdagi, I.G.; Silgu, M.A.; Celikoglu, H.B.: Adaptive signal control to enhance effective green times for pedestrians: a case study. Transp. Res. Procedia **47**, 704–711 (2020)
11. Silgu, M.A.; Akyol, G.; Celikoglu, H.B.: Analysis on pedestrian green time period: preliminary findings from a case study. In: International Conference on Computer Aided Systems Theory, pp. 121–128, Springer (2019)
12. Stevanovic, A.; Martin, P.T.; Stevanovic, J.: VISSIM-based genetic algorithm optimization of signal timings. Transp. Res. Rec. **2035**(1), 59–68 (2007)

13. "Brian" Park, B.; Yun, I.; Ahn, K.: Stochastic optimization for sustainable traffic signal control. Int. J. Sustain. Transp. **3**(4), 263–284 (2009)

14. Yang, Z.; Benekohal, R.F.: Use of genetic algorithm for phase optimization at intersections with minimization of vehicle and pedestrian delays. Transp. Res. Rec. **2264**(1), 54–64 (2011)

15. Gao, K.; Zhang, Y.; Zhang, Y.; Su, R.; Suganthan, P.N.: Meta-heuristics for bi-objective urban traffic light scheduling problems. IEEE Trans. Intell. Transp. Syst. **20**(7), 2618–2629 (2018)

16. Stevanovic, A.; Stevanovic, J.; Zhang, K.; Batterman, S.: Optimizing traffic control to reduce fuel consumption and vehicular emissions: integrated approach with VISSIM, CMEM, and VISGAOST. Transp. Res. Rec. **2128**(1), 105–113 (2009)

17. Stevanovic, A.; Stevanovic, J.; So, J.; Ostojic, M.: Multi-criteria optimization of traffic signals: mobility, safety, and environment. Transp. Res. Part C Emerg. Technol. **55**, 46–68 (2015)

18. Abou-Senna, H.; Radwan, E.: VISSIM/MOVES integration to investigate the effect of major key parameters on CO_2 emissions. Transp. Res. Part D: Transp. Environ. **21**, 39–46 (2013)

19. Jamshidnejad, A.; Papamichail, I.; Papageorgiou, M.; De Schutter, B.: A mesoscopic integrated urban traffic flow-emission model. Transp. Res. Part C Emerg. Technol. **75**, 45–83 (2017)

20. Xu, J.; Hilker, N.; Turchet, M.; Al-Rijleh, M.-K.; Tu, R.; Wang, A.; Fallahshorshani, M.; Evans, G.; Hatzopoulou, M.: Contrasting the direct use of data from traffic radars and video-cameras with traffic simulation in the estimation of road emissions and pm hotspot analysis. Transp. Res. Part D: Transp. Environ. **62**, 90–101 (2018)

21. Jin, J.; Ma, X.: A multi-objective agent-based control approach with application in intelligent traffic signal system. IEEE Trans. Intell. Transp. Syst. **20**(10), 3900–3912 (2019)

22. Pham, D.; Karaboga, D.: Intelligent Optimisation Techniques: Genetic Algorithms, Tabu Search, Simulated Annealing and Neural Networks. Springer Science & Business Media, Berlin (2012)

23. Karaboga, D.: An idea based on honey bee swarm for numerical optimization. Technical Report-TR06, Erciyes University, Engineering Faculty. Tech. Rep, Computer Engineering Department (2005)

24. Liang, X.; Guler, S.I.; Gayah, V.V.: Traffic signal control optimization in a connected vehicle environment considering pedestrians. Transp. Res. Rec. **2674**(10), 499–511 (2020)

25. Liang, X.; Guler, S.I.; Gayah, V.V.: Decentralized arterial traffic signal optimization with connected vehicle information. J. Intell. Transp. Syst. **27**(2), 145–160 (2023)

26. Niels, T.; Mitrovic, N.; Dobrota, N.; Bogenberger, K.; Stevanovic, A.; Bertini, R.: Simulation-based evaluation of a new integrated intersection control scheme for connected automated vehicles and pedestrians. Transp. Res. Rec. **2674**(11), 779–793 (2020)

27. Chen, R.; Hu, J.; Levin, M.W.; Rey, D.: Stability-based analysis of autonomous intersection management with pedestrians. Transp. Res. Part C: Emerg. Technol. **114**, 463–483 (2020)

28. Liu, H.; Gayah, V.V.: A novel max pressure algorithm based on traffic delay. Transp. Res. Part C Emerg. Technol. **143**, 103803 (2022)

29. Liu , H.; Gayah, V.V.: Total-delay-based max pressure: a max pressure algorithm considering delay equity. Transportation Research Record, p. 03611981221147051 (2023)

30. Tsitsokas, D.; Kouvelas, A.; Geroliminis, N.: Two-layer adaptive signal control framework for large-scale dynamically-congested networks: combining efficient max pressure with perimeter control. Transp. Res. Part C Emerg. Technol. **152**, 104128 (2023)

31. Manual, H.C.: "Hcm2010". Transportation Research Board, vol. 1207. National Research Council, Washington (2010)

32. Akcelik, R.: Traffic Signals: Capacity and Timing Analysis (1981)

33. Deb, K.; Pratap, A.; Agarwal, S.; Meyarivan, T.: A fast and elitist multiobjective genetic algorithm: NSGA-II. IEEE Trans. Evol. Comput. **6**(2), 182–197 (2002)

34. Mannering, F.L.; Washburn, S.S.: Principles of Highway Engineering and Traffic Analysis. John Wiley & Sons, Hoboken (2020)

35. Silgu, M.A.; Celikoglu, H.B.; Clustering traffic flow patterns by fuzzy c-means method: some preliminary findings. In: Computer Aided Systems Theory-EUROCAST: 15th International Conference, Las Palmas de Gran Canaria, Spain, February 8–13, 2015, Revised Selected Papers 15. vol. 2015. pp. 756–764, Springer (2015)

36. Demiral, C.; Celikoglu, H.B.: Application of ALINEA ramp control algorithm to freeway traffic flow on approaches to Bosphorus strait crossing bridges. Procedia Soc. Behav. Sci. **20**, 364–371 (2011)

37. Abuamer, I.M.; Celikoglu, H.B.: Local ramp metering strategy ALINEA: microscopic simulation based evaluation study on Istanbul freeways. Transp. Res. Procedia **22**, 598–606 (2017)

38. Silgu, M.A.; Muderrisoglu, K.; Unsal, A.H.; Celikoglu, H.B.: Approximation of emission for heavy duty trucks in city traffic. In: 2018 IEEE International Conference on Vehicular Electronics and Safety (ICVES), pp. 1–4, IEEE (2018)

39. PTV, Ptv vissim 10 user manual. PTV AG: Karlsruhe, Germany (2018)

40. Wiedemann, R.: Simulation des strassenverkehrsflusses (1974)

41. Helbing, D.; Molnar, P.: Social force model for pedestrian dynamics. Phys. Rev. E **51**(5), 4282 (1995)

42. The United States Environmental Protection Agency. Exhaust emission rates for light-duty onroad vehicles in MOVES3' (2020)

43. Akyol, G.; Goncu, S.; Silgu, M.A.; Celikoglu, H.B.: A bi-objective traffic signal optimization model for mixed traffic concerning pedestrian delays. In: Proceedings of 25th Euro Working Group on Transportation Meeting (2024)

44. Miettinen, K.: Nonlinear Multiobjective Optimization, vol. 12. Springer Science & Business Media, Berlin (1999)

45. Pareto, V.: Cours d'économie Politique, vol. 1. Librairie Droz, Genève (1964)

46. Zou, W.; Zhu, Y.; Chen, H.; Zhang, B.: Solving multiobjective optimization problems using artificial bee colony algorithm. Discrete Dyn. Nat. Soc. **2011**, 1–37 (2011)

47. Akbari, R.; Hedayatzadeh, R.; Ziarati, K.; Hassanizadeh, B.: A multi-objective artificial bee colony algorithm. Swarm Evol. Comput. **2**, 39–52 (2012)

48. Li, J.-Q.; Han, Y.-Q.: A hybrid multi-objective artificial bee colony algorithm for flexible task scheduling problems in cloud computing system. Clust. Comput. **23**(4), 2483–2499 (2020)

49. Park, B.; Messer, C.J.; Urbanik, T.: Traffic signal optimization program for oversaturated conditions: genetic algorithm approach. Transp. Res. Rec. **1683**(1), 133–142 (1999)

50. Yun, I.; Park, B.: Stochastic optimization for coordinated actuated traffic signal systems. J. Transp. Eng. **138**(7), 819–829 (2012)

51. Karaboga, D.; Gorkemli, B.; Ozturk, C.; Karaboga, N.: A comprehensive survey: artificial bee colony (ABC) algorithm and applications. Artif. Intell. Rev. **42**, 21–57 (2014)

52. Daamen, W.; Buisson, C.; Hoogendoorn, S.P.: Traffic simulation and data: validation methods and applications. CRC Press, Boca Raton (2014)

53. Webster, F.V.: "Traffic signal settings," Tech. Rep., (1958)

54. Koonce, P.; Rodegerdts, L.: "Traffic signal timing manual." United States. Federal Highway Administration, Tech. Rep., (2008)

55. Coello, C.A.C.; Cortés, N.C.: Solving multiobjective optimization problems using an artificial immune system. Genet. Program Evolvable Mach. **6**, 163–190 (2005)

56. Ren, Y.; Jin, H.; Zhao, F.; Qu, T.; Meng, L.; Zhang, C.; Zhang, B.; Wang, G.; Sutherland, J.W.: A multiobjective disassembly planning for value recovery and energy conservation from end-of-life products. IEEE Trans. Autom. Sci. Eng. **18**(2), 791–803 (2020)